China Petroleum Processing and Petrochemical Technology

Catalyst Research Volume 23, Issue 2, November 2023 Pp. 3932-3946

DESIGN OF A MODE-SELECTIVE FIBER COUPLER FOR CONVERSION OF SPATIAL VECTOR MODES

Sampathi Pidishetti
Department of Physics, University College of Science, Osmania, University, Hyderabad, Telngana-500 007, India.

Shankar P
School of Technology, Woxsen University, Telangana-502345, India.

Shaik Ahmed
School of Technology, Woxsen University, Telangana-502345, India.

Ram Soorat
School of Technology, Woxsen University, Telangana-502345, India.

D. Karuna Sagar
Department of Physics, University College of Science, Osmania, University, Hyderabad, Telngana-500 007, India.

***Corresponding Author**; Shankar P
E-mail: pd.shankara@gmail.com

Abstract –
We present our experimental results on the design and characterization of an all-fiber device based on the mode selective fiber coupler (MSFC) composed using a standard step-index single mode and a few-mode fiber for the generation of the first group of higher orders modes (HOMs) in the few-mode fiber. Our design involves a systematic simulation study on a tapered fiber for mitigating the inevitable issue of mode coupling due to the closed effective index (n_{eff}) of HOMs. By tapering the multimode step-index fiber appropriately, a large difference of Δn_{eff} ~$4x10^{-3}$ between selected HOMs is achieved to avoid the mode coupling without significant power leakage loss in the tapering process. The cut-off tapering diameter limit is estimated to be 2.2 μm, below which higher mode leakage is observed. From these simulation studies, the design parameters are optimizedand experimentally fabricated a special cascaded-coupler design that not only simplifies the fabrication but also enables the wavelength-modulated switchable generation of HOMs with ~90% coupling efficiency with negligible insertion loss. Such wavelength modulated switchable modes with vector characteristics find potentially be used in chemical sensing applications, especially for petroleum processing via identifying petrochemicals such as methane, propane, and hydrogen etc. In addition, these vector modes find significant applications for quantum communication, quantum imaging and optical tweezers as well.

Catalyst Research Volume 23, Issue 2, November 2023 Pp. 3932-3946

Keywords – Fiber Optics, Fiber Spatial Mode, Fiber Couplers, All-fiber, Fiber Device.

1. INTRODUCTION

Optical fiber plays a crucial role in optical communication networks, primarily relying on all-fiber components [1–4]. Single-mode fibers, which guide only one spatial mode, are nearing their maximum transmission capacity. To address this capacity limit, various strategies have been optimized, such as wavelength-division multiplexing (WDM) and polarization-division multiplexing (PDM) [5–7]. Presently, space division multiplexing (SDM) is gaining attention to boost the data-carrying capacity of optical fibers. SDM using fiber or waveguide designs capable of guiding multiple higher-order modes (HOMs), as opposed to single-mode waveguides, which are inherently limited to one spatial mode. Leveraging the spatial dimension as an additional degree of freedom significantly increases the number of data channels that can potentially be used for carrying information independently [5–7]. Apart from these applications, exploitation of the HOMs in fiber has been of great interest for more than three decades due to their promising abilities for numerous applications [8–10] in mitigating non-linear effects in high-power fiber lasers, surface plasmons excitation, material processing, optical tweezers, and high dimensional quantum communication [9,11–16]. In addition, the wavelength modulated switchable mode generating devices find significant applications in chemical sensing applications in petroleum processing through identifying petrochemicals such as methane, propane, and hydrogen etc.

The mode (de)multiplexing component plays a crucial role in generating, sorting, and maintaining the integrity of the HOMs within the communication link. In addition, the capability of optical devices that generate HOMs with high-quality spatial field and polarization characteristics is highly important even for non-communication applications as well. The spatial light modulators (SLMs), q-plates, vortex/spiral phase plates, and forked holograms are commonly used components for generating and sorting the HOMs for classical and quantum fiber networks based on HOMs [6,17–19]. However, these components are non-compatible with all fiber-based systems and suffer from limitations such as low efficiency, restricted bandwidth, scalability challenges, and large size, making them incompatible with fiber networks. Furthermore, these devices can only manage one higher-order mode at a time, and as the number of modes increases, their complexity and susceptibility to alignment issues also rise. As a result, there is a strong emphasis in current research on enhancing existing technologies and developing novel types of such devices.

To implement SDM effectively in future fiber optic networks, fiber-based components are being designed for compatibility with existing telecommunication systems. Although waveguide-based approaches have made significant progress in recent years [5–7], fiber-based solutions still hold promise for the future and are actively under development. In this context, the development of compact all-fiber methods for efficiently generating and sorting HOMs holds significant importance and is currently a subject of intensive research efforts. However, realizing HOMs in fiber is not as straightforward as in free space as detailed below.

The mode solutions of a fiber result in scalar and vector modes, determined by the fiber's guiding

properties, depending on whether the scalar or vector wave treatment is applied, respectively. The scalar modes are characterized by uniform linear polarization (LP), referred to as LP modes, whereas vector modes exhibit spatially varying polarization states, as shown in Figure 1. Vector modes are further identified as HE, EH, and cylindrical vector modes (TE-transverse electric and TM-transverse magnetic), depending on their electric (E) and magnetic (H) field combinations. Furthermore, fiber supports HOMs as a linear combination of a basis set of modes. For instance, if selected HOMs combination with $\pi/2$ phase difference results in an orbital angular momentum mode (OAM). Such OAM modes derived from the linear combination of LP basis modes result in linearly polarized OAM modes, while those obtained from vector basis combination led to circular polarized or vector-OAM modes. It is important to note that OAM modes with circular polarization additionally process the spin-angular momentum (SAM = ±1), thereby resulting in the spin-orbit coupling. OAM modes composed using the LP-scalar basis are susceptible to strong mode coupling due to birefringent perturbations and mode degeneracy, limiting their suitability for various classical and quantum applications. In contrast, OAM modes or HOMs based on the vector basis provide access to manipulate the polarization in the modes, exhibiting pure quantum characteristics with proving to access the high dimensionality of light. This enhances their applications by fully exploiting the maximum available degree of freedom related to polarization, particularly in quantum systems.

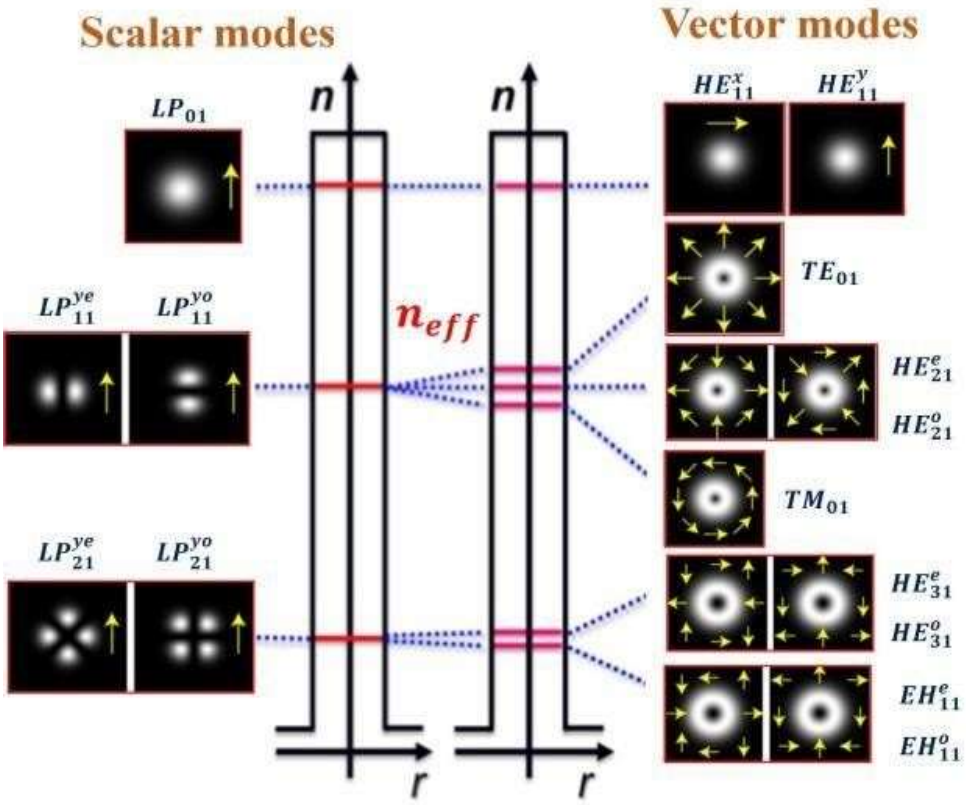

Figure 1: Scalar and vector modes in the optical fiber: PL- linearly polarized modes, n_{eff} - effective refractive index of fiber.

Catalyst Research Volume 23, Issue 2, November 2023 Pp. 3932-3946

While HOMs with pure vector/polarization characteristics offer a full spectrum of benefits, all-fiber devices rely on the special design of the fibers that support HOMs. Such design constraints arise due to the inevitable degeneracy of modes in standard few-mode fibers. In an optical fiber, light can propagate through different paths or modes, each characterized by a unique spatial distribution of the electromagnetic field. The degeneracy of fiber modes refers to the phenomenon where multiple modes within the optical fiber exhibit the same propagation characteristics, such as the same propagation constant or n_{eff}. In other words, these modes propagate with almost the same propagation constants, consequently they cannot be easily distinguished based on their individual characteristics. Due to the symmetry of certain fiber refractive index profiles, multiple modes can share the same set of characteristics. This degeneracy becomes significant when these modes have the same effective refractive index, making it challenging to isolate and manipulate individual modes. The wavelength (λ) dependent propagation constant (β) of modes that related to neff is expressed as follows:

$$\beta(\lambda) = \frac{2\pi}{\lambda} n_{eff} \qquad (1)$$

The presence of degenerate modes in optical fibers can complicate the design and optimization of fiber-based devices, as it becomes more challenging to control and utilize specific modes for desired applications. Researchers and engineers often need to carefully consider and manage the degeneracy of fiber modes to enhance the performance and reliability of optical communication systems and other fiber-optic devices. Thanks to research in fiber design, various specially designed fibers are used for minimizing the mode coupling by lifting the degeneracy between the constituent modes [20,21]. Nevertheless, these fibers are complicated in design and require highly sophisticated processing methods. Leveraging recent advances in such specialty fibers, all fiber mode selective fiber coupler (MSFC) has been reported to generate vector-HOMS and OAM modes [22– 24]. However, the specialty fibers make the device fabrication complicated and sensitive to the critical aliment of the fiber during the device fabrication. Further, these fibers also limit scalability as they are designed to support a specific number of HOMs or OAMs. In this context, as for fiber methods for generating HOMs or OAM modes, various approaches have been explored, including semi-fiber and all-fiber devices such as fiber gratings, micro-structured fibers, mode-selective couplers, photonic lanterns, and fiber-integrated phase plates. However, these methods often face challenges related to efficiency, reliability, bandwidth, scalability, and the purity of generated OAM modes. Although, a photonic lantern is a commercial-grade device used for generating and sorting LP modes, is not capable of handling vector modes and its complex design limit customization. In contrast, MSFCs offer versatility, scalability, and ease of customization with standard and specialty fibers. Importantly, MSFCs are capable of not only generating but also sorting HOMs or OAM modes composed of both vector and scalar basis sets, depending on the fibers used in their design. However, it's worth noting that, except for generating the first-order OAM state, MSCs have not been explored for sorting them with the vector mode basis.

Most of the applications, for instance, optical communication, require all-fiber devices for not only generating HOMs but also modes switching. The MSFCs mechanism has been the potential method to efficiently generate HOMs via all-fiber methods as demonstrated in[23,25]. Most of these previous MSFCs were designed using special fibers with complex index profiles to ensure not only the generation of different types of HOMs but also propagate them with high modal purity [22,23,26]. However, fabrication of MSFCs using such fiber is highly difficult and is efficiency limited [14,27,28]. The design of MSFCs with standard commercial fibers, yet with outstanding performance in not only generating but also switching HOMs is worth exploring as investigated here [8,9].

Here, we present our experimental results on the design and characterization of an MSFC using a standard step-index single mode (SMF) and a few-mode fiber (FMF) for the generation of HOMs. In our design of MSFC, we mainly address two critical issues: mitigating the degeneracy of selected modes and their selective coupling via MSFC design. Furthermore, we demonstrate a wavelength-modulated switchable excitation of HOMs via a special cascaded-coupler design of MSFC. The selection of FMF fiber not only simplifies the fabrication complexity but also generates stable HOMs with a high coupling efficiency of ~90% and with negligible insertion loss. The spatial polarization of generated HOMs is measured via polarization analysis measurements. First, we present our simulation studies on addressing the degeneracy problem of modes via fiber tapering. Subsequently, the design of the proposed MSFC for selective coupling and wavelength-modulated switching of spatial HOMs with vector characteristics is presented, as detailed below.

2. DEGENERACY OF FIBER MODES AND FIBER TAPERING

The following presents our simulation results on investigating the tapered fibers for lifting the degeneracy between the constituent HOMs in a standard multimode step-index fiber to avoid the mode coupling. Our approach makes use of large neff difference induced by strong guidance of HOMs resulting from the fiber tapering. The large effective index difference $\Delta n_{eff} = 3x10^{-3}$ is achieved for the lowest tapered diameter of 2.2 μm and is two orders of magnitude higher as compared to that of HOMs in the un-tapered fiber $\Delta n_{eff} \sim 10^{-5}$. The cut-off taper diameter limit is estimated through the modal field distribution in a tapered fiber. Though tapered fibers are reported for increasing the mode area [29,30], our approach on lifting the degeneracy between the HOMs using the tapered fiber is the first of its kind to the best of our knowledge. As such, this approach not only carries a significant interest for its simplest alternative to lift the degeneracy for mitigating the mode coupling but also for its expected application in the selective launching of HOMs into any fiber to avoid complicated approaches presented in [27,31, 32].

Catalyst Research Volume 23, Issue 2, November 2023 Pp. 3932-3946

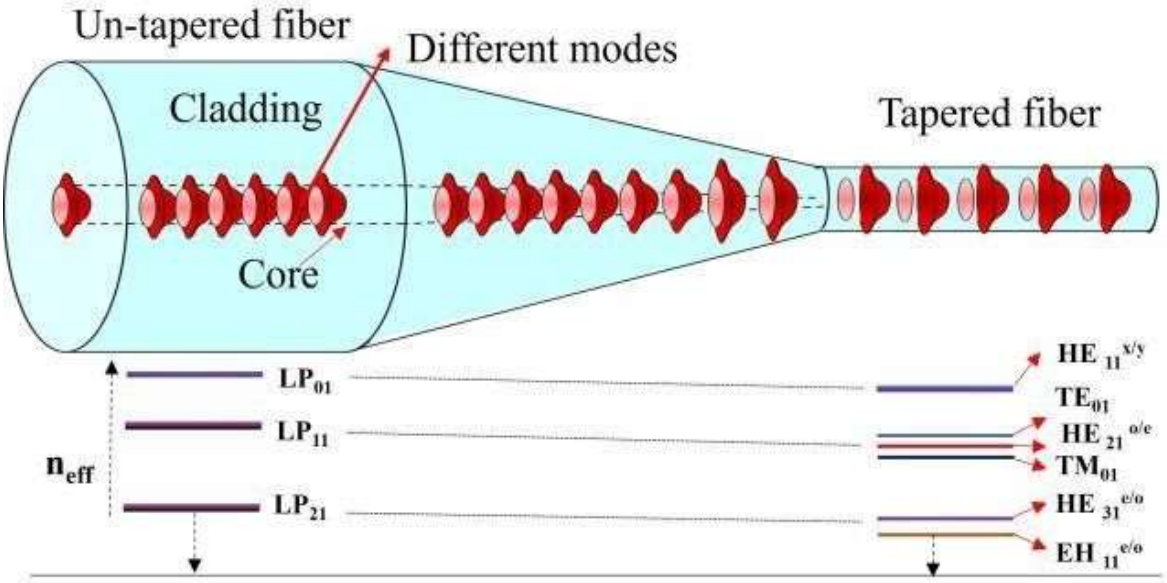

Figure 2: The different modes and their effective index (n_{eff}) in tapered and non-tapered fiber. neff of LP and vector modesare represented with horizontal lines.

modes are appropriate for weakly guiding fiber (un-taperedcase), we consider the natural vector modes in our simulations as they are suitably used in practical applications, and to compare them in un-tapered and tapered fiber.

Figure 2 shows the schematic representation of the effective index of different modes in the tapered and un-tapered fiber. The neff for LP modes and vector modes is indicated with horizontal lines in both regions of the fiber. The mode in the un-tapered fiber is denoted in the form of LP modes as it is the weakly guiding case, while modes in the tapered fiber are shown as vector modes as it is the strongly guiding scenario. As can be noticed, the neff of modes of each LP-modes group in the un-tapered region appears to be a single line due to the close propagation constant of LP modes, while the same lines are splatted, indicating that the propagation constants modes in the tapered fiber are separated, as interpreted via the simulations results below.

First, we performed simulation on a selected un-taperedfiber and calculated the n_{eff} of first 10 vector modes as a function of wavelength for the range of 1.55 µm to 1.60 µm as shown in Figure 3. It can be seen from Figure 3 that the neff of different modes is almost indistinguishable for un-tapered fiber.

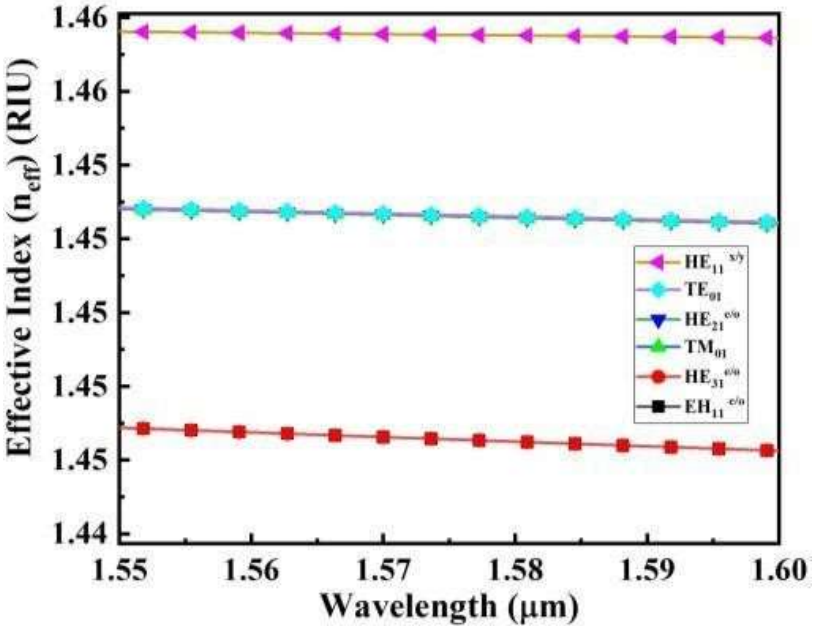

Figure 3: n_{eff} of different modes as a function of wavelength for an un-tapered fiber.

The Δneff calculated between the constituent mode as a function of wavelength for the first (TE_{01}, $HE_{21}^{e/o}$, $TM0_1$) and second ($HE_{31}^{e/o}$ and $EH_{11}^{e/o}$) HOM groups is $3.12x10^{-5}$ and $1.6x10^{-7}$, respectively. Since, neff of modes in each group are close to each other, they propagate with almost similar or closest propagation constant ($\beta = 2\pi/\lambda.n_{eff}$). This indicates that modes are vulnerable to prominent mode coupling in the un-tapered fiber [20].

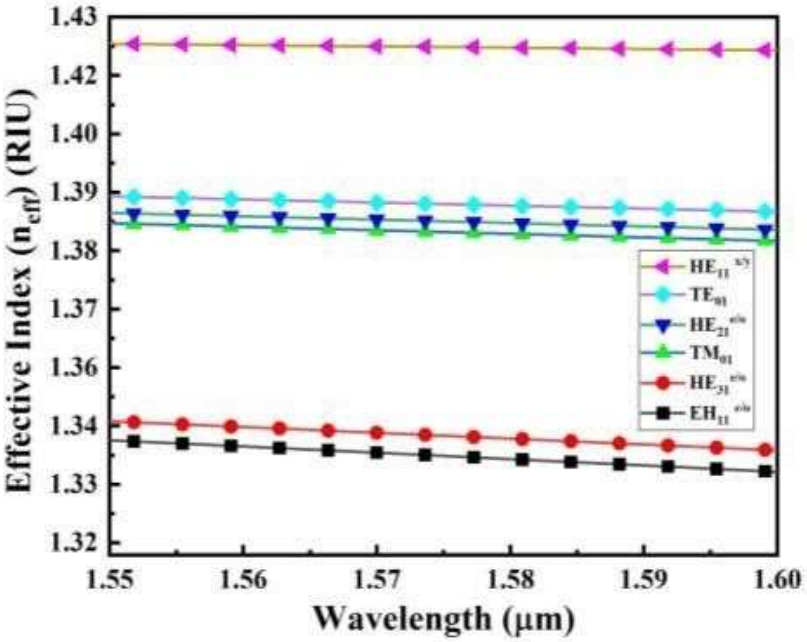

Figure 4: Effective index n_{eff} of different modes as a function of wavelength in a 2.2 μm taper (cladding) diameter.

Catalyst Research Volume 23, Issue 2, November 2023 Pp. 3932-3946

A standard multi-mode step-index fiber with core/cladding diameters 10.2 μm /125 μm, and corresponding refractive index 1.46/1.444 is used in our simulations. With numerical aperture (NA) of 0.241 and V-number of 4.98 this fiber supports up to ~12 modes including all degenerate vector counterparts at 1.55 μm wavelength. We use COMSOL Multiphysics® eigen mode solver to perform the simulations. Though, LPlm. In the subsequent simulations, the neff of the HOMs is calculated as a function of taper diameter. It is observed that the Δn_{eff} increased between the HOMs as tapering diameter of the fiber decreases. Furthermore, the neff of the HOMs calculated as a function of wavelength for taper diameter of 2.2 μm are shown in Figure 4. The Δn_{eff} calculated between modes in the first and second HOM groups is $3.4x10^{-3}$ and $4x10^{-3}$ RUI respectively, which is two orders of magnitude higher than that of HOMs in un- tapered fiber. It is known that the Δn_{eff} higher than the order of 10^{-4} between the constituent modes can significantly avoid the modal coupling [20,21]. These results indicate that tapering the fiber can significantly avoid the mode coupling by lifting the degeneracy between the modes. However, we believe that these tapered fibers are applicable for only selective excitation of modes [29–31] and studies on modal coupling behavior [33], but not for propagation. Further, it is possible that HOMs can be lossy at lower taper diameters due to the power leakage. Thus, we calculated the mode fields for tapering diameter of 2.2 μm for each selected HOMs and found out that below 2.2 um of tapering diameter, the HOMs are lossy. This indicates that 2.2 μm is the lower cut-off limit of tapering diameter for the selected HOMs in this fiber. From these simulation studies, it is clear that the tapering process involved in the proposed MSFC enables selective coupling of modes despite a step-index few-mode fiber is used in the design. By leveraging such advantage of selective coupling of modes, we further optimize the design parameters to achieve the switching of modes as described below.

3. DESIGN OF A MODE SELECTIVE FIBER COUPLER

A standard step-index fiber (25/125 μm, NA 0.12, FS Inc. call no. 35275) that supports few-modes, and a standard SMF-28 (Thorlabs Inc.) at 1550 nm wavelength were used to fabricate the proposed MSFC and optimize the coupler parameters to excite switchable HOMs. The index profile analysis of selected FMF revealed that this fiber possesses the sufficient index separation (in the order of Δn_{eff}~10^{-4}) between the supporting HOMs so that modes do not couple each other after they get coupled. Since the degeneracy between the different polarized modes is removed, selective excitation and stability of generated HOMs can be achieved.

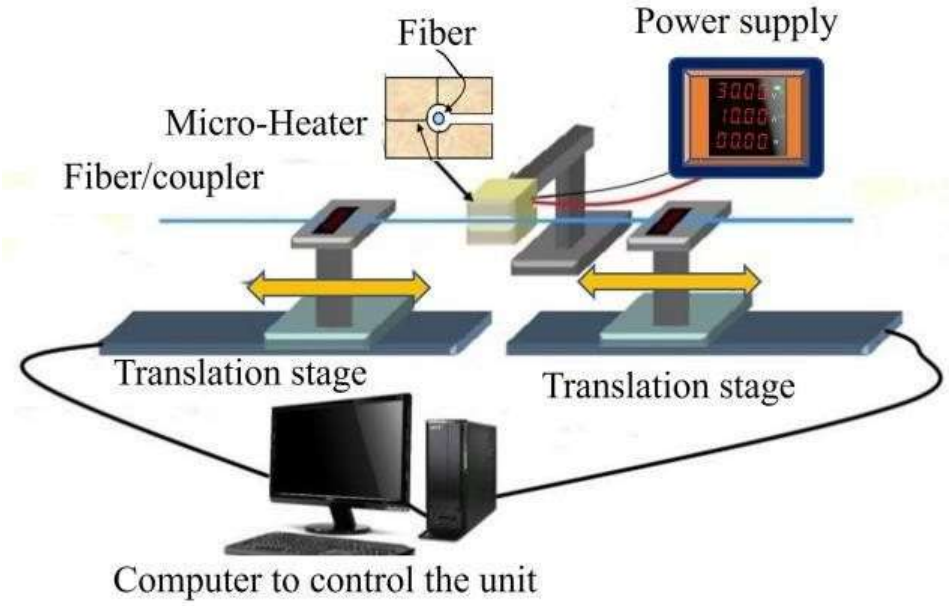

Figure 5: Schematic representation of coupler fabrication tapering-rig.

The n_{eff} of the HE_{11} in the SMF is different from that of HOMs in the FMF fiber. Thus, selected modes must be phase matched, which is studiedusing COMSOL Multiphysics® eigenmode solver and found out the required tapering ratio ($\rho = r_{SMF}/r_{FMF}$) of selected fibers [22,23]. First, SMF was adiabaticallypre-tapered at ~1400ºC to a radius that is calculated based on the simulations, using the tapering rig shown in Figure 5. The pre-tapered SMF was longitudinally aligned with the un-tapered, straight FMF fiber without any twists, as previously reported in [22,23]. The degree of fusion is optimized to obtain a cascaded fusedcoupler and the HE_{11} mode in the SMF couples into a selected HOMs in the FMF to which it is phase matched [22,23]. The tapering and fusing werestopped when the power measured out of the FMF fiber was maximized, which is measured to be ~90%.

Further, the wavelength modulated switching of HOMs is achieved by optimizing the coupling length of the coupler which is 18.2mm. At this coupling length, the coupler performance of modes coupling becomes highly wavelength dependent thereby tuning the wavelength results in phase change of selected modes. This design results in coupling of HE_{11} mode into a different HOMsto which it is phase matched at tuned wavelength. As the coupler design employed a weakly fusing technique,the polarization of coupled HOMs is well preserved thereby resulting coupled modes to maintain the vector characteristics. The fabricated coupler was carefully packed and characterized further as explained below.

Unpolarized light from a tunable 1550-nm laser source was launched into the SMF input port of the coupler Figure 6. The SMF was subjected to circular bendsto strip out if any higher order mode was present before the fused region of the device. The output beam from theFMF fiber was collimated using an appropriate lens (f =12mm) and the field patterns were imaged using a CCD camera. Inset in the Figure 6 shows a clear doughnut pattern out of the FMF fiber port, as a

Catalyst Research Volume 23, Issue 2, November 2023 Pp. 3932-3946

function of tuned wavelength, when the polarizer is not present in the beampath before the camera. The doughnut intensity distribution qualitatively suggests that the input HE_{11} mode substantially get coupled to the target HOMs.

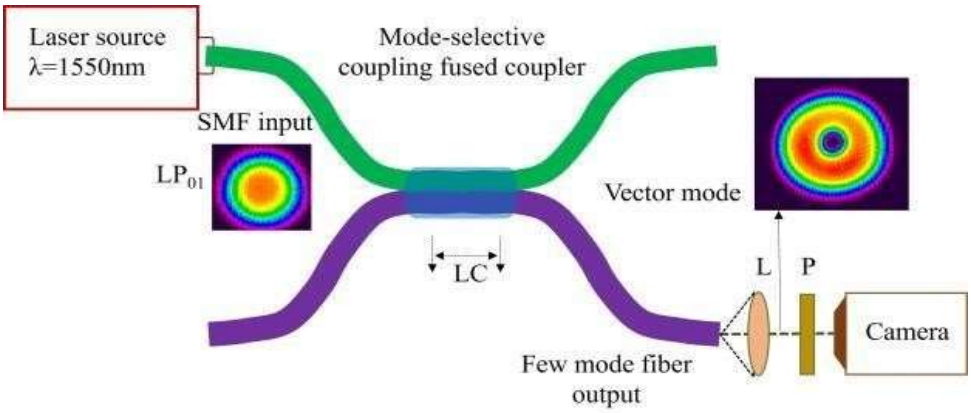

Figure 6 (a): Experimental setup for characterizing the coupler. Inset: intensity profile of different modes out of the mode selective coupler. LC: the coupling length of MSFC. L- lens and P-polarizer.

Further, the wavelength of the source has been turned to three (1550, 1552.5 and 1555 nm) different wavelengths and the polarization of the output beam is analyzed using a polarizer components as detailed below, based on the reported in [22].

A polarization analyzer was inserted in the path of the free-space collimated beam. The transmitted beam out of polarizer was measured as a function of the rotation angle of the polarization axis of polarizer.

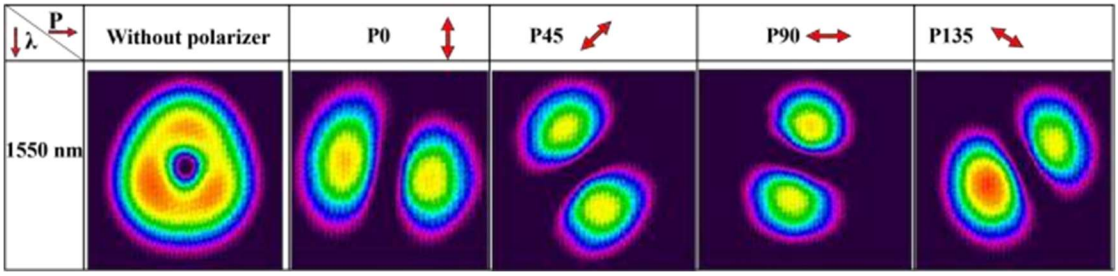

Figure 7: Experimentally generated one of the HOMs at 1.55 µm. Images of mode intensity distribution without polarizer and with rotation angle of polarizer: confirming the generated mode possesses the vector characteristics as spatial polarization varied across the mode's cross-section.

The appearance of the dark line across the beam cross section, after passing through the polarizer suggests that the polarization state of the generated beams is inhomogeneous. Further rotation of analyzer axis through 0^0-135^0 at selected discrete angles, the two-lobed field pattern on the CCD also rotated along the same rotation direction as shown in Figure 7. Such behavior is the signature of the spatially varying polarization of mode coupler HOMs which confirms that the

generated mode possesses the vector characteristics as polarization varies spatially. Furthermore, based on the lobe like patterns of beam, it can be concluded that the coupler mode is of TE_{01}.

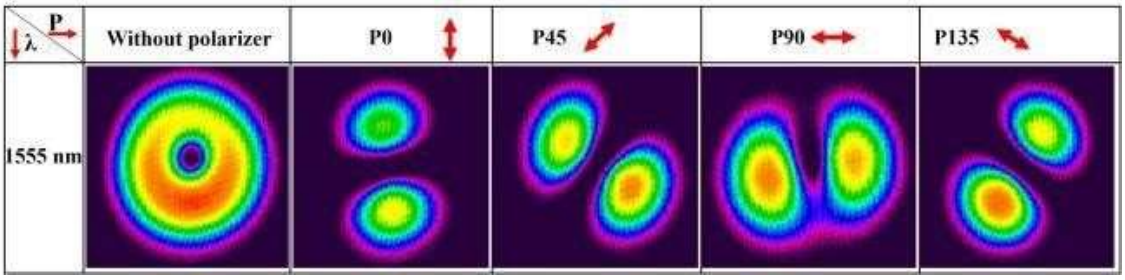

Figure 8: Experimentally generated one of the HOMs at 1.555 μm. Images of mode intensity distribution without polarizer and with rotation angle of polarizer: confirming that the generated mode possesses the vector characteristics as polarization varies spatially.

Further, the wavelength of input light into SMF is tuned to 1.555 μm. As usual, the intensity patterns as a function of different polarization angles are measured, as shown in Figure 8. This pattern is indicative of the spatially changing polarization in the mode coupler's higher-order modes (HOMs), affirming that the resulting mode exhibits vector characteristics with polarization variations across space. Moreover, by observing the lobe-like patterns, it can be deduced that the mode generated by the coupler corresponds to TM_{01} and is different from the mode generated at 1.55 μm. The observed intensity CCD image profiles confirm that the generated beams possess different polarization at different wavelengths, as the lobe pattern is different for different polarizer axis for the two selected wavelengths. Moreover, the changing structure of spatial polarization of the modes as a function of input tuned wavelength, further confirms the switching of the generated modes. Therefore, by modulating the input wavelength, the modes can be switched. Such wavelength modulated switchable vectors modes have high potential for chemical sensing applications [34-38]. Especially the fiber-based devices are especially suitable for remote sensing in toxic chemical environments, chemical chambers with limited access [34, 35]. With such potential, this result carries significant importance in sensing petrochemicals and petroleum processing applications [34, 35]. The petrochemicals such as methane, propane, and hydrogen etc., can be identified based on their wavelength dependent response to vector characteristics of each wavelength modulated switchable modes [34, 35].

To conclude, our study showcases a method for generating switchable Higher Order Modes (HOMs), like TE_{01}, and TM_{01}. It is achieved through a straightforward mode-selective coupler design using a standard step-index single mode (SMF) and a few-mode fiber. The degenerate properties of the selected modes are studied via simulations and found that the tapering process used in fabricating proposed MSCF helps in lifting the degeneracy between the modes. The unique cascaded-coupler design allows for the wavelength-modulated switchable generation of HOMs with an efficiency approximately equal to 90%, all while maintaining the fabrication process simple. These uncomplicated and highly effective all-fiber devices demonstrate exceptional performance and hold significant potential for various applications, including optical

communication, particle manipulation, and mode switching. Ongoing efforts involve further analysis to obtain spatially resolved polarization through Stok's polarization parameters measurement, and results on the polarization analysis will be reported elsewhere separately.

6. CONCLUSION

A switchable generation of HOMs with vector characteristics via a design of a mode-selective fiber coupler is demonstrated. The design involves a single mode and a standard step-index few-mode fiber. In this work, we presented our simulation results on the tapered fibers for lifting the degeneracy between the constituent HOMs in a standard multimode step-index fiber to achieve selective coupling. The large effective index difference $\Delta n_{eff} = 4x10^{-3}$ is achieved for the lowest tapered diameter of 2.2 μm and is two orders of magnitude higher as compared to that of HOMs in the un-tapered fiber $\Delta n_{eff} \sim 10^{-5}$. As such, our approach not only carry a significant interest for its simplest alternative to lift the degeneracy for mitigating the mode coupling but also for its expected application in selective launching of HOMs into any fiber to avoid complicate approaches. The special cascaded-coupler design enables the wavelength modulated switchable generation of HOMs with ~90% efficiency while keeping the fabrication simple. Such simple and highly efficient, yet with outstanding performance, all- fiber based devices are highly potential for various application such as optical communication, particle manipulation and modes switching. Realizing the full potential of quantum technologies crucially relies on the development of devices that can manipulate and propagate quantum states efficiently. In this context, the reported research carries significant importance by providing an all-fiber device solution capable of multiplexing multiple vector modes effectively utilizing a vector basis set for even OAM modes, ensuring suitability not only for classical applications but also for quantum applications. This research work has potential to bridge the gap between fiber networks and compatible all-fiber devices, offering a commercially viable, versatile solution to replace bulky and inefficient non-fiber systems in classical and quantum research. Hence, exploring the design of MSFCs using standard step-index fiber that can offer accessibility of vector characteristics of the generated HOMs finds many applications.

ACKNOWLEDGEMENT

Authors thank Prof. Gilberto Brambilla, Optoelectronics Research Centre, University of Southampton for facilitating the labs to carry out the experiments.

REFERENCES

1. J. Wang, S. Chen, and J. Liu, "Orbital angular momentum communications based on standard multi- mode fiber (invited paper)," APL Photonics **6**(6), 060804 (2021).
2. A. Manzalini, "Topological Photonics for Optical Communications and Quantum Computing," Quantum Reports **2**(4), 579–590 (2020).
3. J. Liu, L. Zhu, A. Wang, S. Li, S. Chen, C. Du, Q. Mo, and J. Wang, "All-fiber pre- and post-data exchange in km-scale fiber-based twisted lights multiplexing," Optics Letters **41**(16), 3896 (2016).

4. A. M. Yao and M. J. Padgett, "Orbital angular momentum: origins, behavior and applications," Adv. Opt. Photon. **3**(2), 161–204 (2011).
5. G. Milione, M. P. J. Lavery, H. Huang, Y. Ren, G. Xie, T. A. Nguyen, E. Karimi, L. Marrucci, D. A. Nolan, R. R. Alfano, and A. E. Willner, "4 × 20 Gbit/s mode division multiplexing over free space using vector modes and a q-plate mode (de)multiplexer," Optics Letters **40**(9), 1980 (2015).
6. J. Wang, Q. Wang, J. Liu, and D. Lyu, "Quantum orbital angular momentum in fibers: A review," AVS Quantum Science **4**(3), 031701 (2022).
7. N. Bozinovic, Y. Yue, Y. Ren, M. Tur, P. Kristensen, H. Huang, A. E. Willner, and S. Ramachandran, "Terabit-Scale Orbital Angular Momentum Mode Division Multiplexing in Fibers," Science **340**(6140), 1545–1548 (2013).
8. S. Ramachandran and P. Kristensen, "Optical vortices in fiber," nanoph **2**(5–6), 455–474 (2013).
9. Y. Shen, S. Pidishety, I. Nape, and A. Dudley, "Self- healing of structured light: a review," J. Opt. **24**(10), 103001 (2022).
10. S. Zhu, S. Pidishety, Y. Feng, S. Hong, J. Demas, R. Sidharthan, S. Yoo, S. Ramachandran, B. Srinivasan, and J. Nilsson, "Multimode-pumped Raman amplification of a higher order mode in a large mode area fiber," Opt. Express, OE **26**(18), 23295–23304 (2018).
11. S. Pidishety, S. Zhu, Y. Feng, B. Srinivasan, and J. Nilsson, "Raman amplification of optical beam carrying orbital angular momentum in a multimode step-index fiber," Opt. Lett., OL **44**(7), 1658–1661 (2019).
12. S. Zhu, S. Pidishety, Y. Feng, S. Hong, J. Demas, R. Sidharthan, S. Yoo, S. Ramachandran, B. Srinivasan, and J. Nilsson, "Multimode-pumped Raman amplification of a higher order mode in a large mode area fiber," Opt. Express, OE **26**(18), 23295–23304 (2018).
13. M. Meier, V. Romano, and T. Feurer, "Material processing with pulsed radially and azimuthally polarized laser radiation," Appl. Phys. A **86**(3), 329– 334 (2006).
14. S. Ramachandran and P. Kristensen, "Optical vortices in fiber," Nanophotonics **2**(5–6), 455–474 (2013).
15. L. Zou, Y. Yao, and J. Li, "High-power, efficient and azimuthally polarized ytterbium-doped fiber laser," Optics Letters **40**(2), 229 (2015).
16. K. J. Moh, X.-C. Yuan, J. Bu, D. K. Y. Low, and R. E. Burge, "Direct noninterference cylindrical vector beam generation applied in the femtosecond regime," Applied Physics Letters **89**(25), 251114 (2006).
17. X. Heng, J. Gan, Z. Zhang, J. Li, M. Li, H. Zhao, Q. Qian, S. Xu, and Z. Yang, "All-fiber stable orbital angular momentum beam generation and propagation,"Opt. Express, OE **26**(13), 17429–17436 (2018).
18. X. Zeng, Y. Li, L. Feng, S. Wu, C. Yang, W. Li, W. Tong, and J. Wu, "All-fiber orbital angular momentum mode multiplexer based on a mode-selective photonic lantern and a mode polarization controller," Opt. Lett., OL **43**(19), 4779–4782 (2018).
19. H. Zhang, B. Mao, Y. Han, Z. Wang, Y. Yue, and Y. Liu, "Generation of Orbital Angular

Momentum Modes Using Fiber Systems," Applied Sciences **9**(5), 1033 (2019).
20. S. Ramachandran, S. Golowich, M. F. Yan, E. Monberg, F. V. Dimarcello, J. Fleming, S. Ghalmi, and P. Wisk, "Lifting polarization degeneracy of modes by fiber design: a platform for polarization- insensitive microbend fiber gratings," Optics Letters **30**(21), 2864 (2005).
21. C. Brunet, P. Vaity, Y. Messaddeq, S. LaRochelle, and L. A. Rusch, "Design, fabrication and validation of an OAM fiber supporting 36 states," Optics Express **22**(21), 26117 (2014).
22. S. Pidishety, B. Srinivasan, and G. Brambilla, "All- Fiber Fused Coupler for Stable Generation of Radially and Azimuthally Polarized Beams," IEEE Photonics Technology Letters **29**(1), 31–34 (2017).
23. S. Pidishety, S. Pachava, P. Gregg, S. Ramachandran, G. Brambilla, and B. Srinivasan, "Orbital angular momentum beam excitation using an all-fiber weakly fused mode selective coupler," Opt. Lett., OL **42**(21), 4347–4350 (2017).
24. S. Pidishety, M. A. Khudus, P. Gregg, S. Ramachandran, B. Srinivasan, and G. Brambilla, "OAM Beam Generation using All-fiber Fused Couplers," in *CLEO: Science and Innovations* (OpticalSociety of America, 2016), pp. STu1F-2.
25. R. Ismaeel, T. Lee, B. Oduro, Y. Jung, and G. Brambilla, "All-fiber fused directional coupler for highly efficient spatial mode conversion," Optics Express **22**(10), 11610 (2014).
26. P. Gregg, P. Kristensen, and S. Ramachandran, "Conservation of orbital angular momentum in air- coreoptical fibers," Optica, OPTICA **2**(3), 267–270 (2015).
27. A. W. Snyder and J. D. Love, *Optical Waveguide Theory* (Springer US, 1984).
28. J. D. Love and N. Riesen, "Mode-selective couplers for few-mode optical fiber networks," Optics Letters **37**(19), 3990 (2012).
29. J. Kerttula, V. Filippov, V. Ustimchik, Y. Chamorovskiy, and O. G. Okhotnikov, "Mode evolution in long tapered fibers with high tapering ratio," Opt. Express, OE **20**(23), 25461–25470 (2012).
30. S. Ravets, J. E. Hoffman, P. R. Kordell, J. D. Wong- Campos, S. L. Rolston, and L. A. Orozco, "Intermodal energy transfer in a tapered optical fiber: optimizing transmission," J. Opt. Soc. Am. A, JOSAA **30**(11), 2361–2371 (2013).
31. W. Q. Thornburg, B. J. Corrado, and X. D. Zhu, "Selective launching of higher-order modes into anoptical fiber with an optical phase shifter," Opt. Lett., OL **19**(7), 454–456 (1994).
32. R. Ismaeel and G. Brambilla, "Removing the Directional Degeneracy of Mode in a Fused-Type Mode Selective Coupler," Journal of LightwaveTechnology **34**(4), 1242–1246 (2016).
33. Z. Ma, G. Prabhakar, P. Gregg, and S. Ramachandran, "Robustness of OAM fiber modes to geometric perturbations," in *Conference on Lasers and Electro- Optics (2018), Paper SW3K.1* (Optical Society of America, 2018), p. SW3K.1.
34. L. Kopf, J. R. D. Ruano, M. Hiekkamäki, T. Stolt, M. J. Huttunen, F. Bouchard, and R. Fickler, "Spectral vector beams for high-speed spectroscopic measurements," Optica, OPTICA 8(6), 930–935 (2021).
35. S. A. Syubaev, A. Y. Zhizhchenko, D. V. Pavlov, S. O. Gurbatov, E. V. Pustovalov, A. P. Porfirev, S. N. Khonina, S. A. Kulinich, J. B. B. Rayappan, S. I. Kudryashov, and A. A.

Kuchmizhak, "Plasmonic Nanolenses Produced by Cylindrical Vector Beam Printing for Sensing Applications," Sci Rep 9(1), 19750 (2019).
36. R. Li, L. Guo, B. Wei, C. Ding, Z. Wu, R. Li, L. Guo, B. Wei, C. Ding, and Z. Wu, "Fiber-Based Cylindrical Vector Beams and Its Applications to Optical Manipulation," in Advances in Optical Fiber Technology: Fundamental Optical Phenomena and Applications (IntechOpen, 2015).
37. D. J. J. Hu, L. Liu, H. Dong, and H. Zhang, "Design of a Broadband Fiber Optic Mode Coupler for Multimode Optical Coherence Tomography," Photonics 10(2), 162 (2023).
38. Q. Zhan, "Cylindrical vector beams: from mathematical concepts to applications," Adv. Opt. Photon., AOP 1(1), 1–57 (2009).